

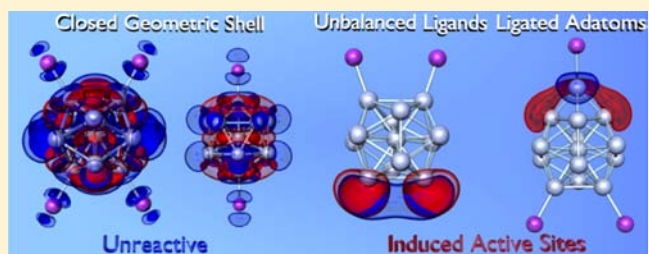
Ligand-Induced Active Sites: Reactivity of Iodine-Protected Aluminum Superatoms with Methanol

Marissa Baddick Abreu, Christopher Powell, Arthur C. Reber, and Shiv N. Khanna*

Department of Physics, Virginia Commonwealth University, Richmond, Virginia 23284, United States

S Supporting Information

ABSTRACT: The quantum states in metal clusters are bunched into electronic shells as in atoms. Ligands including halogens or thiols modify the electronic structure through bonding, resulting in stable clusters with filled electronic shells that are resistant to oxygen etching. We demonstrate that the stabilization afforded by ligands is partially confounded because the ligands perturb the charge density of the metallic core, inducing Lewis acid–base sites that make the cluster reactive in a protic environment. We demonstrate the importance of induced active sites by studying the reactivity of methanol with two classes of iodine-passivated aluminum cluster anions: $\text{Al}_{13}\text{I}_x^-$, which has a closed geometric shell, and $\text{Al}_{14}\text{I}_y^-$, which has an adatom-decorated core. Two adjacent ligands on the closed geometric shell of Al_{13}^- activate the cluster, while in $\text{Al}_{14}\text{I}_3^-$ the I induces an active site on the adatom, making the cluster reactive, explaining ligand-protected clusters' preference for closed geometric shells.



INTRODUCTION

Due to quantum confinement, the states in compact metallic clusters are grouped into bunches or shells similar to those in atoms.¹ A spherical jellium model, wherein the cluster is replaced by a uniform positive background the size of the cluster, provides a simplified model of the confined nearly free electron gas, and the electronic states may be assigned effective N and L quantum numbers ordering as 1S, 1P, 1D, 2S, 1F, 2P, ..., granting the clusters an electronic shell structure reminiscent of atoms.^{2,3} Extensive work over the past 25 years has shown that the stability and the electronic, magnetic, optical, and chemical behaviors of the clusters can be rationalized within such a model.^{4–7} Clusters with filled electronic shells exhibit enhanced stability as seen through mass spectra and chemical inertness as seen through reactivity with etchants such as oxygen.^{8,9} Clusters with unfilled shells acquire a filled shell through the addition of a precise number of ligands or electrons, allowing the application of a simple valence model. This “superatom concept” serves as an organizational principle which identifies clusters with a well-defined valence and categorizing them, forming a third dimension to the periodic table.

One way to passivate metallic clusters and control their electronic structure is to attach ligands. Successful ligands include thiols,^{10–17} phosphines,^{18–21} and halogens.^{22–26} These ligands undergo electronegative bonding with the metallic core of the cluster, perturbing the electronic structure of the cluster. Ligand-protected clusters serve as building blocks in numerous nanomaterials, and their stability is often reconciled by ligands granting the cluster a closed electronic shell through covalent or ionic bonding.²⁴ We define a closed electronic shell cluster as

having an unusually large highest occupied molecular orbital (HOMO)–lowest unoccupied molecular orbital (LUMO) gap for a metallic cluster due to filling all of the closely packed orbitals with the same effective N and L quantum numbers, in analogy with atoms. We note that clusters with nonspherical geometries may induce unusually large HOMO–LUMO gaps within subshells in some rare instances.^{27,28} Clusters with closed electronic shells may be identified by a strong resistance to reaction with molecular oxygen due to spin accommodation.⁹ For example, the Al_{14}^- cluster has 43 valence electrons, 3 more than the closed shell at 40 electrons. The addition of three iodine ligands results in an $\text{Al}_{14}\text{I}_3^-$ with a closed electronic shell analogous to that at 40 valence electrons. Experiments reveal that Al_{14}^- reacts rapidly with oxygen, while $\text{Al}_{14}\text{I}_3^-$ is resistant toward etching by oxygen, confirming the closed electronic shell.

Electronegative ligands stabilize clusters by granting them a closed electronic shell; however, the ligands may distort the even distribution of charge on the metallic core, resulting in active sites. Complementary active sites govern the reactivity of aluminum clusters with water; clusters that are spherical and have an even distribution of charge are resistant to water and methanol etching, while clusters with edges and defects are reactive due to the ensuing uneven distribution of charge.^{29–35} The reacting species are marked by nonuniform charge density distribution, where one Al atom acts as a Lewis acid and a nearby Al atom acts as a Lewis base. These complementary active sites are indicated by the LUMO and HOMO of the

Received: September 24, 2012

Published: November 26, 2012

cluster. The close proximity of the Lewis acid–base pair is effective in breaking the O–H bond of water and methanol. Our hypothesis is that adding electronegative iodine ligands to aluminum clusters may induce an uneven distribution of charge, modifying the reactivity.

In this work, we investigate how active sites could be induced in metallic clusters by attaching ligands. The synthesis of ligand-protected clusters is often performed in a protic environment in solvents such as H₂O and CH₃OH, so the ability of a cluster to be etched by protic molecules is a critical factor in identifying enduring clusters. We demonstrate the intriguing induction of active sites through first-principles studies of the reactivity of Al₁₃I_x[−] and Al₁₄I_y[−] clusters with methanol. Al₁₃[−] has a closed electronic shell of 40 electrons, and previous studies on Al₁₃I_x[−] clusters have shown that the clusters retain their closed electronic shell and their approximately icosahedral metallic core. These findings were confirmed by experiments showing that Al₁₃I_{2n}[−] clusters were resistant to etching by oxygen. Here we demonstrate how such clusters with closed electronic shells can break O–H bonds through repositioning of I atoms to generate induced active sites, although such clusters with a single unbalanced ligand are not found to have enhanced reactivity. For Al₁₄I_y[−], the clusters have a closed electronic shell at *y* = 3 and 5, and the metallic core may be characterized as an icosahedral core with an adatom. Here, we show that the electron-withdrawing nature of iodine, specifically in the case of Al₁₄I₃[−], successfully induces active sites which enable reaction with methanol, even though the cluster has a closed electronic shell and does not react with oxygen. These studies show that the distribution of charge density can produce new reactive patterns different from those caused by electronic shell closure and caused by the electronegative ligand, inducing an active site.

THEORETICAL METHODS

All calculations were performed using a first-principles molecular orbital approach, in which the molecular orbitals are represented by a linear combination of atomic orbitals centered at the atomic sites, within a gradient-corrected density functional theory. Actual calculations were performed using the NRLMOL set of codes,^{36–38} wherein the atomic orbitals are expressed as a linear combination of Gaussian orbitals located at the atomic sites in the cluster. The basis set consisted of 6s, 5p, and 3d functions for Al, 8s, 7p, and 5d functions for I, 4s, 3p, and 1d functions for H, and 5s, 4p, and 3d functions for both C and O. The generalized gradient approximation proposed by Perdew, Burke, and Ernzerhof (PBE) was used to incorporate exchange and correlation.³⁹ Transition-state geometries were found using a linear transit approach along the O–H bond. The ground-state geometries were obtained by moving atoms in the direction of forces until the forces dropped below a threshold value of 0.05 eV/Å. The search for ground states included several starting geometries, and the absorption site for methanol included investigation of numerous absorption sites.

RESULTS AND DISCUSSION

Al₁₃I_x[−] (*x* = 0–4). We first examined the ground-state structures and corresponding wave functions of the frontier orbitals for Al₁₃I_x[−], as shown in Figure 1. (See the Supporting Information for coordinates.) All of the clusters maintain an approximately icosahedral core of aluminum atoms, with the iodine bonding to external sites. The electronic shell structure of metallic clusters often results in a number of degenerate or nearly degenerate states. To identify Lewis base active sites, we have plotted in red all occupied orbitals that are within 82 meV

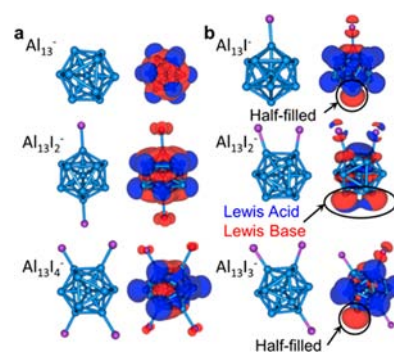


Figure 1. Geometric structures and frontier orbitals of (a) Al₁₃[−], Al₁₃I₂[−], and Al₁₃I₄[−] and (b) Al₁₃I[−], Al₁₃I₃[−], and a higher energy isomer of Al₁₃I₂[−]. Al atoms are light blue, and I atoms are purple. The HOMOs are shown in red, and the LUMOs are shown in blue.

in energy of the HOMO. To identify Lewis acid sites, we have plotted in blue all unoccupied orbitals that lie close in energy to the LUMO. Also, when considering the Lewis acidity of a cluster, we identified the lowest completely unoccupied orbital, as an orbital in which the LUMO is half-filled may not serve as a Lewis acid.

Al₁₃[−], shown in Figure 1a, is a canonical closed electronic shell cluster with a HOMO–LUMO gap of 1.87 eV, and the frontier orbitals are delocalized evenly over the 12 surface atoms of the cluster. As each surface atom is equivalent, no site on Al₁₃[−] will serve as a superior or inferior donor of electrons relative to other sites. Al₁₃I₂[−] and Al₁₃I₄[−] also have symmetrical frontier orbital distributions and maintain large HOMO–LUMO gaps of 1.70 and 1.65 eV, respectively, explaining their resistance to reactivity with oxygen. Al₁₃I₂[−] and Al₁₃I₄[−] have balanced I ligands that lie in antipodal positions on diametrically opposite sides of the icosahedral core. The remaining accessible metal sites are equivalent in Al₁₃I₂[−] and quite similar in Al₁₃I₄[−], so these clusters also have an even distribution of charge. The clusters with an odd number of iodine ligands, Al₁₃I[−] and Al₁₃I₃[−], have unbalanced I ligands and have unsymmetrical frontier orbital charge distribution (Figure 1b). In both clusters a distinct lobe appears on the cluster directly opposite the unbalanced iodine atoms. The lobe comes from the half-filled HOMO and marks the most favorable site for an additional iodine ligand. The orbital is the 2P delocalized orbital that has been pushed up in energy by the interaction of the antipodal iodine with the 2P delocalized orbital. The unoccupied frontier orbital charge densities are still distributed symmetrically about the core of the clusters. An isomer of Al₁₃I₂[−], in which the two iodine atoms are arranged on adjacent aluminum atoms, shows a distinct pair of Lewis acid and Lewis base sites opposite the two iodine atoms. The sites are marked by the HOMO and LUMO, indicating a potential pair of complementary active sites.

The reactivity of these clusters with methanol was characterized by four quantities. The binding energy, *E_B*, is the nondissociative binding energy of methanol bound to the cluster and is a measure of the Lewis acidity of the cluster as shown in the following equation:

$$E_B = E(\text{CH}_3\text{OHAl}_{13}\text{I}_x^-)_{\text{ads}} - (E(\text{Al}_{13}\text{I}_x^-) + E(\text{CH}_3\text{OH})) \quad (1)$$

The greater the binding energy, the more charge transfer from the lone pair of methanol to the cluster and hence the stronger the Lewis acidity of the cluster. The transition-state energy, *E_T*,

is the energy of the transition state relative to the separated cluster and is an indicator of reactivity as shown in the following equation:

$$E_T = E(\text{CH}_3\text{OHA}l_{13}I_x^-)_{\text{TS}} - (E(\text{Al}_{13}I_x^-) + E(\text{CH}_3\text{OH})) \quad (2)$$

Previous studies have found that clusters which have transition-state energies greater than 0.10 eV more than those of the separated reactants reveal negligible reactivity in a gas-phase reaction chamber on the time scale of flow tube reactions, so the transition energy is the critical parameter for predicting reactivity in gas-phase studies.^{29,30,35} The third quantity used to characterize the reactivity is the activation energy, or potential energy barrier, E_A , which is the difference between the total energy of the bound complex and the total energy of the transition-state complex, as seen in the following equation:

$$E_A = E(\text{Al}_{13}I_x^- + \text{CH}_3\text{OH})_{\text{TS}} - E(\text{CH}_3\text{OHA}l_{13}I_x^-)_{\text{ads}} \quad (3)$$

This value may be of most interest in the liquid phase as the binding energy may be rapidly dissipated by the solvent, so the reactivity will most likely follow the Arrhenius law with E_A serving as the activation energy. The final-state energy, E_R , is the relative energy of the final product of the reaction. E_R is found using the following equation:

$$E_R = E(\text{CH}_3\text{OHA}l_{13}I_x^-)_{\text{diss}} - (E(\text{Al}_{13}I_x^-) + E(\text{CH}_3\text{OH})) \quad (4)$$

The values of E_B , E_T , E_R , and E_A for $\text{Al}_{13}I_x^-$ are listed in Table 1. Note that although the values of E_B and E_R are negative, this

Table 1. Binding, Transition-State, Reaction, and Activation Energies for the Reaction of Methanol with $\text{Al}_{13}I_x^-$

cluster	E_B (eV)	E_T (eV)	E_R (eV)	E_A (eV)
Al_{13}^-	-0.15	0.25	-0.77	0.40
Al_{13}I^-	-0.14	0.23	-1.34	0.37
$\text{Al}_{13}\text{I}_2^-$	-0.29	0.20	-0.85	0.49
$\text{Al}_{13}\text{I}_2^-_{\text{adj}}$	-0.67	-0.42	-2.14	0.25
$\text{Al}_{13}\text{I}_3^-^a$	-0.29	0.21	-1.34	0.50
$\text{Al}_{13}\text{I}_4^-^a$	-0.27	0.26	-0.72	0.53

^aReaction pathways are shown in the Supporting Information.

implies that the complex has a lower total energy than the cluster and methanol molecule separated. We will refer to the absolute values of these quantities in the discussion to follow. Using the E_B , E_T , and E_R values, we produced interpolated curves to represent the reaction pathways, as shown in Figure 2.

In the first test of ligand-induced reactivity, we compared the reactivity of Al_{13}^- with that of Al_{13}I^- . Figure 2a shows the lowest energy reaction pathway for Al_{13}^- with methanol. The positive value of +0.25 eV for E_T , shown in Table 1, indicates that the cluster is expected to have minimal reactivity in gas-phase experiments, which has been confirmed by experiment.³³ This result is explained by the remarkably symmetrical charge density distribution of the frontier orbitals on Al_{13}^- . The low 0.15 eV binding energy reveals that Al_{13}^- is a poor Lewis acid because the cluster's closed electronic shell makes it resistant to accepting charge. The E_A for the reaction is 0.40 eV, which we will use for comparison with other clusters. In Figure 2b, we see the result of adding an iodine ligand. The E_T value is +0.23 eV, demonstrating that the cluster is predicted to be resistant to reactivity with methanol in gas-phase experiments. In addition,

the binding energy is 0.14 eV, virtually identical to that of Al_{13}^- , so the Lewis acidity of the cluster was not enhanced by ligation. The E_A is reduced from 0.40 to 0.37 eV on the addition of I, which shows a minimal increase in reactivity. Although the addition of an iodine atom to the Al_{13}^- cluster did disrupt the symmetrical arrangement of the occupied frontier orbital charge density, by inducing HOMO density on the opposite side of the cluster, this site is only half-filled and does not make a strong Lewis base. Furthermore, the unoccupied frontier orbital charge density is still diffuse, so there is no complementary Lewis acid site. The Lewis base site does increase the final energy after the O–H bond is broken from 0.77 eV in Al_{13}^- to 1.34 eV in Al_{13}I^- in a process analogous to the antipodal arrangement of I in $\text{Al}_{13}\text{I}_2^-$. We observed the same unreactive behavior for the ground states of $\text{Al}_{13}\text{I}_2^-$ as shown in Figure 2c. The binding energy in $\text{Al}_{13}\text{I}_2^-$ is enhanced by the formation of a hydrogen bond between the iodine atom and the alcohol. The E_T is +0.20 eV, making the cluster unreactive with methanol in gas-phase reactions, and the E_A increases from 0.40 to 0.49 eV on the addition of the two balanced iodine ligands, with the increase being due to the high-lying transition state and the hydrogen bond with iodine enhancing the binding energy. We also studied the reactivity for $\text{Al}_{13}\text{I}_3^-$ and $\text{Al}_{13}\text{I}_4^-$ in Table 1 and Figure S1 (Supporting Information). These clusters also show weak Lewis acidity, as demonstrated by low binding energies, which can be attributed to the electronic shell closure, making the cluster resistant to accepting charge. $\text{Al}_{13}\text{I}_3^-$ and $\text{Al}_{13}\text{I}_4^-$ have E_T values of +0.21 and +0.26 eV, making them unreactive in gas-phase studies. The E_A values are found to be 0.50 and 0.53 eV as shown in Table 1, which further confirms that their reactivity in the liquid phase is expected to be similar to that of Al_{13}^- .

To determine the effect of ligand placement on cluster reactivity, we explored the reaction pathway of a higher energy isomer of $\text{Al}_{13}\text{I}_2^-$ with methanol. This isomer has two iodine atoms bonded to adjacent aluminum atoms with a potential complementary active site on the opposite side of the cluster. As shown in Table 1 and Figure 2d, the cluster has an E_T of -0.42 eV, showing that it is highly reactive in the gas phase. Furthermore, the binding energy is 0.67 eV, more than 2 times the binding energy of $\text{Al}_{13}\text{I}_2^-$ in the ground state, indicating that this higher energy isomer is a strong Lewis acid site. The HOMO–LUMO gap decreases to 0.74 eV, indicating that the adjacent ligands partially disrupt the closed electronic shell of the cluster, making it a stronger Lewis acid. In addition, the E_A , at 0.25 eV, is about 60% that of the ground state. Methanol donates an electron pair to one of the aluminum atoms directly opposite the iodine atoms: this is the Lewis acid site. Then the O–H bond is broken as the hydrogen bonds to the second aluminum atom opposite the iodine atoms: this is the Lewis base site. This demonstrates that the presence of two adjacent iodine ligands induces a fully unoccupied frontier orbital on the opposite side of the cluster, activating a strong Lewis acid site and making the cluster reactive with methanol.

$\text{Al}_{14}I_y^-$ ($y = 0-5$). We examined the ground-state structures and the corresponding frontier orbitals for the $\text{Al}_{14}I_y^-$ series and present them in Figure 3. (See the Supporting Information for coordinates.) As with the $\text{Al}_{13}I_x^-$ series, the charge densities of the occupied orbitals are represented by a red isosurface, while the unoccupied orbitals are represented by a blue isosurface. The $\text{Al}_{14}I_y^-$ clusters all contain a compact 14-atom metallic core that may be described as an icosahedron with an adatom decorating one triangular face of the icosahedron. It is worth

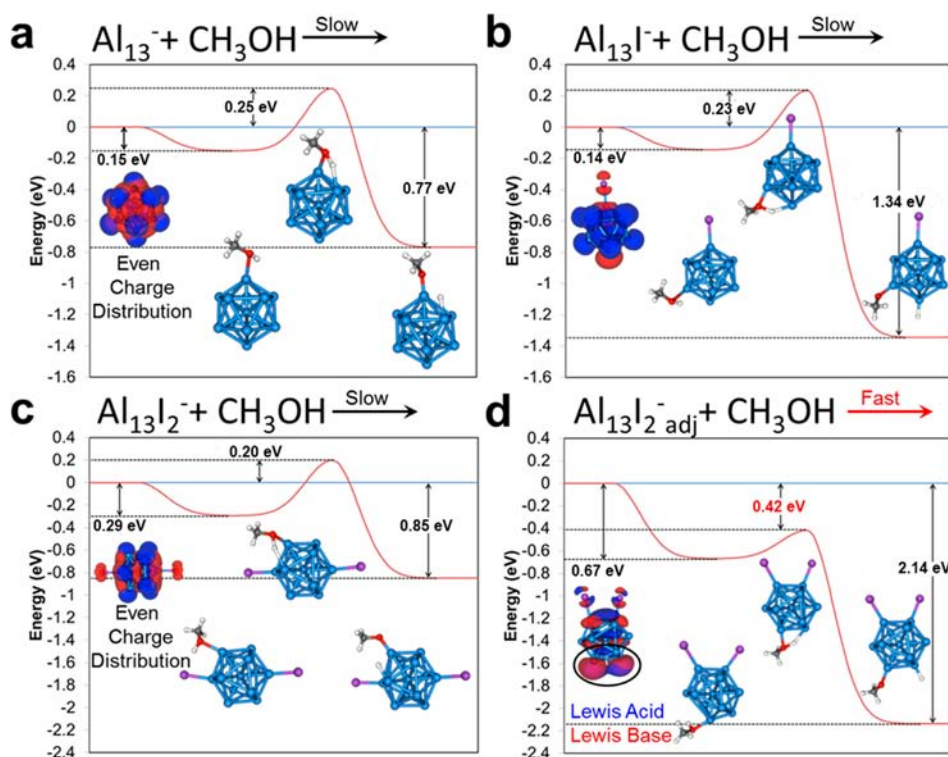


Figure 2. Lowest energy reaction pathways with methanol for the ground states of (a) Al_{13}^- , (b) Al_{13}I^- , and (c) $\text{Al}_{13}\text{I}_2^-$ and for (d) a higher energy isomer of $\text{Al}_{13}\text{I}_2^-$, with I atoms on adjacent sites. Al is shown in light blue, and I is shown in purple. HOMOs are red, and LUMOs are blue.

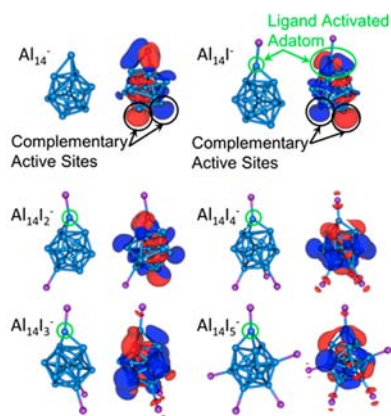


Figure 3. Geometric structures and frontier orbitals of the $\text{Al}_{14}\text{I}_y^-$ series: Al_{14}^- , Al_{14}I^- , $\text{Al}_{14}\text{I}_2^-$, $\text{Al}_{14}\text{I}_3^-$, $\text{Al}_{14}\text{I}_4^-$, and $\text{Al}_{14}\text{I}_5^-$. Al atoms are light blue, and I atoms are purple. The HOMOs are red, and the LUMOs are blue.

noting that the adatom-decorated core results in an electronic spectrum with much less degeneracy than that of the approximately spherical $\text{Al}_{13}\text{I}_x^-$ series. The $\text{Al}_{14}\text{I}_y^-$ clusters have viable complementary active sites that could lead to possible reaction, including at the adatom site and at sites opposite the adatom. How does the presence of the adatom affect the reactivity of the ligand-protected aluminum clusters?

We found that $\text{Al}_{14}\text{I}_3^-$ reacts with methanol at the adatom site despite the fact that $\text{Al}_{14}\text{I}_3^-$ has a closed electronic shell and is resistant to oxygen etching. As Figure 4a illustrates, the oxygen on methanol donates its electron pair to the adatom, and the hydrogen then bonds to an adjacent aluminum atom which is marked by an occupied orbital density: complementary active sites in action. The nondissociative binding energy,

shown in Table 2, is 0.44 eV, significantly higher than the binding energies found on ground-state geometries in the $\text{Al}_{13}\text{I}_x^-$ series. The E_T is -0.20 eV, and the energy barrier, E_A , is only 0.24 eV, resulting in a rapid gas-phase reaction and enhanced liquid-phase reactivity. $\text{Al}_{14}\text{I}_3^-$ is unreactive with methanol at sites on the icosahedral core, whether that site is ligated with iodine, as in Figure 4b, or is an all-metal site, as in Figure 4c. Reactions at these sites have positive E_T values of +0.13 and +0.36 eV, respectively, and E_A values significantly larger than Al_{13}^- . In particular, the reaction of methanol at an all-metal site on the icosahedral core reveals unexpected results. Despite a high binding energy, which is an indication that it serves as a strong Lewis acid site, the energy barrier, E_A , of 0.71 eV prevents the rapid breaking of the O–H bond. A ligand is expected to reduce the reactivity of a metal site due to steric effects; however, we find that, in a cluster with a ligand bound to an adatom, the adatom becomes activated by the ligand. Identical results were found for $\text{Al}_{14}\text{I}_5^-$ (Figure S2, Supporting Information), which is also stable to oxygen etching, as well as for $\text{Al}_{14}\text{I}_2^-$ and $\text{Al}_{14}\text{I}_4^-$, which are not stable to O_2 due to the clusters' doublet spin states (Figure S2).²³ As Table 2 shows, these clusters which are reactive at the adatom site have low E_A values, similar to the E_A of the higher energy isomer of $\text{Al}_{13}\text{I}_2^-$ and in most cases lower than this. This confirms the importance of the geometric structure of the metallic core, even in clusters with ligand protecting groups.

Because the clusters $\text{Al}_{14}\text{I}_y^-$ ($y = 2-5$) were all reactive at an adatom site with a ligand, we next explored if the ligand was a necessary feature to enhance the reactivity, or if a bare adatom would have the same effect. To test this, we studied the reaction of Al_{14}^- and Al_{14}I^- with methanol. As Figure 4d shows, Al_{14}^- will react with methanol at the complementary active sites on the side of the cluster opposite the adatom. However, slow reactivity is observed at the adatom (Figure 4e). The energy

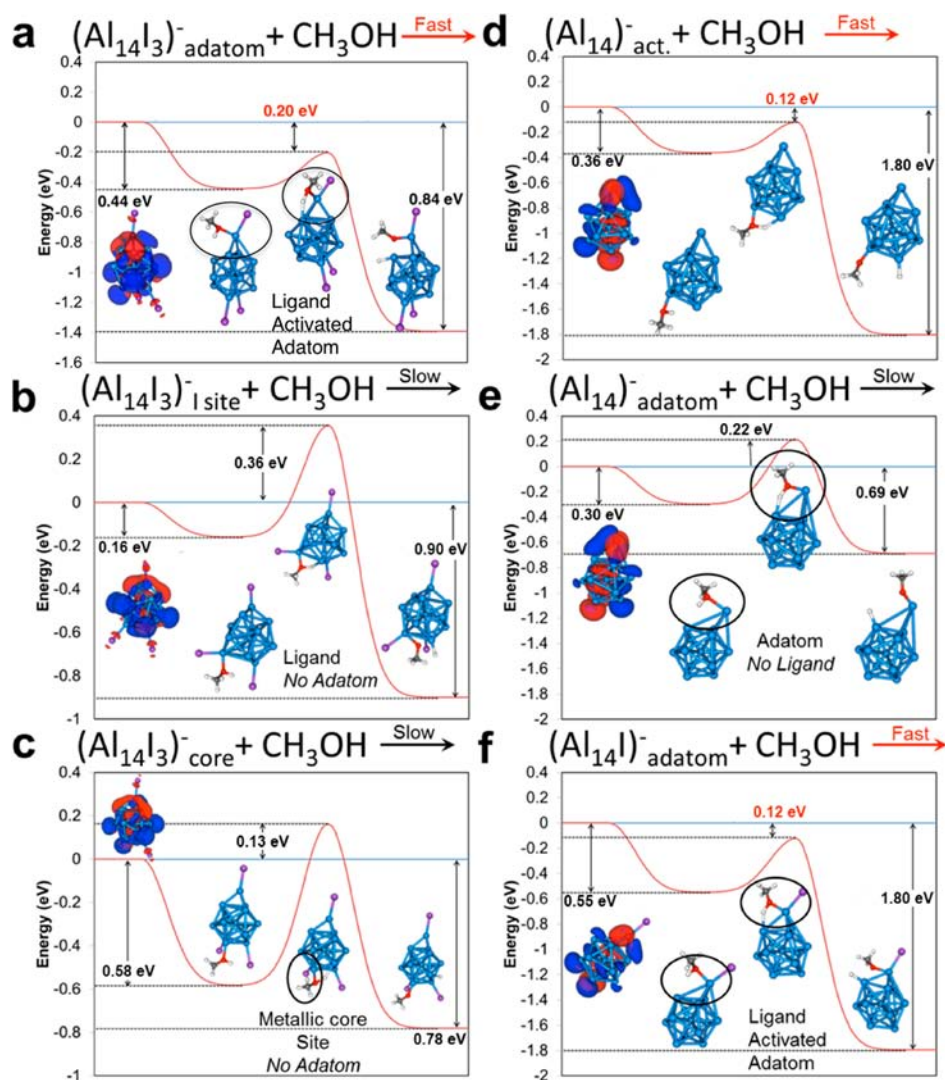


Figure 4. Selected reaction pathways of $\text{Al}_{14}\text{I}_y^-$ clusters with methanol. Reaction pathways with methanol for $\text{Al}_{14}\text{I}_3^-$ at three different sites on the cluster: (a) the adatom, (b) an aluminum atom bonded to an iodine atom on the core, and (c) an all-metallic site on the core. Reaction pathways with methanol for Al_{14}^- at (d) an active site on the core and (e) the adatom. (f) Reaction pathway with methanol for Al_{14}I^- at the adatom site. Al atoms are shown in light blue, and I atoms are shown in purple. The HOMO density is red, while the LUMO density is blue.

Table 2. Binding, Transition-State, Reaction, and Activation Energies for the Reaction of Methanol with $\text{Al}_{14}\text{I}_x^-$

cluster	E_B (eV)	E_T (eV)	E_R (eV)	E_A (eV)
Al_{14}^- act	-0.36	-0.12	-1.80	0.24
Al_{14}^- adatom	-0.30	0.22	-0.69	0.52
Al_{14}I^- adatom	-0.55	-0.12	-1.80	0.43
$\text{Al}_{14}\text{I}_3^-$ adatom	-0.44	-0.20	-0.84	0.24
$\text{Al}_{14}\text{I}_3^-$ I site	-0.16	0.36	-0.90	0.52
$\text{Al}_{14}\text{I}_3^-$ core	-0.58	0.13	-0.78	0.71
$\text{Al}_{14}\text{I}_2^-$ adatom ^a	-0.41	-0.23	-1.12	0.18
$\text{Al}_{14}\text{I}_4^-$ adatom ^a	-0.40	-0.17	-0.95	0.23
$\text{Al}_{14}\text{I}_5^-$ adatom ^a	-0.38	-0.18	-1.35	0.20

^aReaction pathways are shown in the Supporting Information.

barrier, E_A , shown in Table 2, to the reaction with methanol at the adatom site of bare Al_{14}^- is 0.52 eV, with an E_T 0.22 eV greater than the initial binding energy. When the adatom is ligated with iodine in Al_{14}I^- , the E_A decreases by 0.09 to 0.43 eV and has an E_T of -0.12 eV, indicating that the adatom is activated by the addition of the ligand (Figure 4f). The binding

energy of methanol to Al_{14}I^- is nearly 2 times as large as the binding energy of methanol to Al_{14}^- , meaning the ligated adatom is a much stronger Lewis acid site than the bare adatom. The electron-withdrawing iodine ligand pulls electron density away from the aluminum adatom, activating it as a Lewis acid site, and as there is a complementary Lewis base site, the reaction proceeds rapidly. This demonstrates that an adatom alone or a ligand on a surface site is insufficient to activate the cluster, while an adatom with a ligand cooperatively activates the cluster.

CONCLUSIONS

Ligands affect the reactivity of the aluminum clusters in unexpected ways. The icosahedral core $\text{Al}_{13}\text{I}_x^-$ clusters did not react with methanol, despite the presence of one unbalanced iodine ligand. Al_{13}^- is an exceptionally poor Lewis acid because it has a closed electronic shell with a set of high-lying LUMOs which enacts an energy penalty when binding to the lone pair on the methanol molecule. While the lowest energy isomer of $\text{Al}_{13}\text{I}_2^-$ is unreactive, if the iodine atoms are found on adjacent aluminum atoms, a complementary active site is induced on the

opposite side of the cluster, resulting in the rapid reaction with methanol. The $Al_{14}I_y^-$ clusters which have an adatom-decorated core cast further light on the effect of ligands on the reactivity. Clusters with iodine ligands bound to the adatom site are reactive at the site, despite the presence of the ligand. The electronically closed shell species $Al_{14}I_3^-$, which is resistant to oxidation by O_2 , reacts with methanol at the adatom site. The adatom site must be ligated with an electron-withdrawing group to activate the cluster. We add that we have recently shown that such complementary active sites can also break carbonyl bonds in formaldehyde. Since the ligands can induce such complementary active pairs, and as ligated clusters can be assembled into nanoassemblies, the present work may open a pathway toward designing nanomaterials that can selectively break polar covalent bonds. These results also explain the tendency of ligand-protected clusters toward compact metallic cores with closed geometric shells.

■ ASSOCIATED CONTENT

● Supporting Information

Coordinates of optimized ground, binding, transition, and final states of $Al_{13}I_x^-$ and $Al_{14}I_y^-$ and reaction pathways of $Al_{13}I_3^-$, $Al_{13}I_4^-$, $Al_{14}I_2^-$, $Al_{14}I_4^-$, and $Al_{14}I_5^-$ with methanol. This material is available free of charge via the Internet at <http://pubs.acs.org>.

■ AUTHOR INFORMATION

Corresponding Author

snkhanna@vcu.edu

Notes

The authors declare no competing financial interest.

■ ACKNOWLEDGMENTS

We gratefully acknowledge financial support from the Air Force Office of Scientific Research through MURI Grant No. FA9550-08-01-0400.

■ REFERENCES

- (1) Castleman, A. W.; Khanna, S. N. *J. Phys. Chem. C* **2009**, *113*, 2664.
- (2) Knight, W. D.; Clemenger, K.; de Heer, W. A.; Saunders, W. A.; Chou, M. Y.; Cohen, M. L. *Phys. Rev. Lett.* **1984**, *52*, 2141.
- (3) Brack, M. *Rev. Mod. Phys.* **1993**, *65*, 677.
- (4) Khanna, S. N.; Jena, P. *Phys. Rev. B* **1995**, *51*, 13705.
- (5) Janssens, E.; Neukermans, S.; Lievens, P. *Curr. Opin. Solid State Mater. Sci.* **2004**, *8*, 185.
- (6) Bréchnignac, C.; Cahuzac, P.; Carlier, F.; de Frutos, M. *Phys. Rev. Lett.* **1990**, *64*, 2893.
- (7) Selby, K.; Kresnin, V.; Masui, J.; Vollmer, M.; de Heer, W. A.; Scheidemann, A.; Knight, W. D. *Phys. Rev. B* **1991**, *43*, 4565.
- (8) Leuchtner, R. E.; Harms, A. C.; Castleman, A. W. *J. Chem. Phys.* **1989**, *91*, 2753.
- (9) Reber, A. C.; Khanna, S. N.; Roach, P. J.; Woodward, W. H.; Castleman, A. W. *J. Am. Chem. Soc.* **2007**, *129*, 16098.
- (10) Moreno, M.; Ibañez, F. J.; Jasinski, J. B.; Zamborini, F. P. *J. Am. Chem. Soc.* **2011**, *133*, 4389.
- (11) Akola, J.; Kacprzak, K. A.; Lopez-Acevedo, O.; Walter, M.; Gronbeck, H.; Hakkinen, H. *J. Phys. Chem. C* **2010**, *114*, 15986.
- (12) Lopez-Acevedo, O.; Tsunoyama, H.; Tsukuda, T.; Hakkinen, H.; Aikens, C. M. *J. Am. Chem. Soc.* **2010**, *132*, 8210.
- (13) Clayborne, P. A.; Lopez-Acevedo, O.; Whetten, R. L.; Gronbeck, H.; Hakkinen, H. *J. Chem. Phys.* **2011**, *135*, 094701.
- (14) Nimmala, P. R.; Dass, A. *J. Am. Chem. Soc.* **2011**, *133*, 9175.
- (15) Zhu, M.; Aikens, C. M.; Hollander, F. J.; Schatz, G. C.; Jin, R. *J. Am. Chem. Soc.* **2008**, *130*, 5883.
- (16) Heaven, M. W.; Dass, A.; White, P. S.; Holt, K. M.; Murray, R. *W. J. Am. Chem. Soc.* **2008**, *130*, 3754.
- (17) Jadzinsky, P. D.; Calero, G.; Ackerson, C. J.; Bushnell, D. A.; Kornberg, R. D. *Science* **2007**, *318*, 430.
- (18) Briant, C. E.; Theobald, B. R. C.; White, J. W.; Bell, L. K.; Mingos, D. M. P. *J. Chem. Soc., Chem. Commun.* **1981**, 201.
- (19) Shichibu, Y.; Negishi, Y.; Watanabe, T.; Chaki, N. K.; Kawaguchi, H.; Tsukuda, T. *J. Phys. Chem. C* **2007**, *111*, 7845.
- (20) Pettibone, J. M.; Hudgens, J. W. *J. Phys. Chem. Lett.* **2010**, *1*, 2536.
- (21) Shafai, G.; Hong, S.; Bertino, M.; Rahman, T. S. *J. Phys. Chem. C* **2009**, *113*, 12072.
- (22) Bergeron, D. E.; Castleman, A. W.; Morisato, T.; Khanna, S. N. *Science* **2004**, *304*, 84.
- (23) Bergeron, D. E.; Roach, P. J.; Castleman, A. W.; Jones, N. O.; Khanna, S. N. *Science* **2005**, *307*, 231.
- (24) Walter, M.; Akola, J.; Lopez-Acevedo, O.; Jadzinsky, P. D.; Calero, G.; Ackerson, C. J.; Whetten, R. L.; Gronbeck, H.; Hakkinen, H. *Proc. Natl. Acad. Sci. U.S.A.* **2008**, *105*, 9157.
- (25) Shichibu, Y.; Suzuki, K.; Konishi, K. *Nanoscale* **2012**, *4*, 4125.
- (26) Jiang, D.; Walter, M. *Nanoscale* **2012**, *4*, 4234.
- (27) Roach, P. J.; Woodward, W. H.; Reber, A. C.; Khanna, S. N.; Castleman, A. W. *Phys. Rev. B* **2010**, *81*, 195404.
- (28) Luo, Z.; Gamboa, G. U.; Smith, J. C.; Reber, A. C.; Revelese, J. U.; Khanna, S. N.; Castleman, A. W. *J. Am. Chem. Soc.* **2012**, *134*, 18973.
- (29) Roach, P. J.; Woodward, W. H.; Castleman, A. W.; Reber, A. C.; Khanna, S. N. *Science* **2009**, *323*, 492.
- (30) Reber, A. C.; Khanna, S. N.; Roach, P. J.; Woodward, W. H.; Castleman, A. W. *J. Phys. Chem. A* **2010**, *114*, 6071.
- (31) Bunker, C. E.; Smith, M. J.; Fernando, K. A. S.; Harruff, B. A.; Lewis, W. K.; Gord, J. R.; Gulians, E. A.; Phelps, D. K. *ACS Appl. Mater. Interfaces* **2010**, *2*, 11.
- (32) Bunker, C. E.; Smith, M. J. *J. Mater. Chem.* **2011**, *21*, 12173.
- (33) Shimojo, F.; Ohmura, S.; Kalia, R. K.; Nakano, A.; Vashishta, P. *Phys. Rev. Lett.* **2010**, *104*, 126102.
- (34) Day, P. N.; Nguyen, K. A.; Pachter, R. *J. Chem. Theory Comput.* **2011**, *8*, 152.
- (35) Reber, A. C.; Roach, P. J.; Woodward, W. H.; Khanna, S. N.; Castleman, A. W. *J. Phys. Chem. A* **2012**, *116*, 8085.
- (36) Pederson, M. R.; Jackson, K. A. *Phys. Rev. B* **1990**, *41*, 7453.
- (37) Jackson, K.; Pederson, M. R. *Phys. Rev. B* **1990**, *42*, 3276.
- (38) Porezag, D.; Pederson, M. R. *Phys. Rev. A* **1999**, *60*, 2840.
- (39) Pedew, J. P.; Burke, K.; Ernzerhof, M. *Phys. Rev. Lett.* **1996**, *77*, 3865.